

Functionalized adamantane: fundamental building blocks for nanostructure self-assembly

J. C. Garcia¹, J. F. Justo², W. V. M. Machado¹, and L. V. C. Assali¹

¹ *Instituto de Física, Universidade de São Paulo,
CP 66318, CEP 05315-970, São Paulo, SP, Brazil*

² *Escola Politécnica, Universidade de São Paulo,
CP 61548, CEP 05424-970, São Paulo, SP, Brazil*

(Dated: August 12, 2009)

Abstract

We report first principles calculations on the electronic and structural properties of chemically functionalized adamantane molecules, either in isolated or crystalline forms. Boron and nitrogen functionalized molecules, aza-, tetra-aza-, bora-, and tetra-bora-adamantane, were found to be very stable in terms of energetics, consistent with available experimental data. Additionally, a hypothetical molecular crystal in a zincblende structure, involving the pair tetra-bora-adamantane and tetra-aza-adamantane, was investigated. This molecular crystal presented a direct and large electronic bandgap and a bulk modulus of 20 GPa. The viability of using those functionalized molecules as fundamental building blocks for nanostructure self-assembly is discussed.

PACS numbers: 81.07.-b,68.65.-k,61.46.-w

I. INTRODUCTION

Carbon is unique in nature because it carries several competing hybridization states for its valence electrons, leading to a number of stable, and sometimes exotic, organized structures. Diamond and graphite crystalline structures, with carbon respectively in sp^3 and sp^2 hybridizations, already present remarkable properties, leading to applications ranging from cutting tools to electronic devices. On the other hand, nanostructured forms of carbon, which have been discovered over the last two decades, could potentially lead to a much wider range of applications in a near future¹. Those nanostructures, that included fullerenes, nanotubes, graphene, nanoribbons, and others, have been the focus of intensive investigation. Fullerenes have been considered as lubricants, nanotubes have been used to build nanodiodes and nanotransistors², and nanoribbons have been considered for molecular electronics³.

Striking developments have been recently attained in building, separating, manipulating, and functionalizing a different class of nanostructured carbon, called diamondoids. They can be described as molecular diamond, with carbon atoms in a diamond-like structure saturated by hydrogen atoms in the surface. Due to the prevailing covalent nature of the interatomic interactions, those molecules carry outstanding stability and rigidity. Adamantane is the smallest diamondoid, with a $C_{10}H_{16}$ configuration, which consists of a single diamond-like carbon cage. Larger diamondoids, such as diamantane, triamantane, and higher polyman-
tanes, are obtained by incorporating additional carbon cages to adamantane.

Diamondoids have been known for almost 100 years, since their discovery in petroleum. The recent identification and separation of higher diamondoids⁴ allowed to envision several applications, such as electron emission devices^{5,6}, chemical sensors⁷, biomarkers⁸, and pharmaceuticals⁹. They have also been considered as building blocks (BBs) to build complex ordered nano-elements with sub-nanometric precision^{10,11}. Using BBs represents a potentially competitive building procedure for industrial applications within a bottom-up approach. BBs can be thought as nanobricks, but manipulating them represents a major challenge. Since adamantane is the smallest diamondoid, it could be considered as a fundamental building block (FBB). Current methods that allow positional control, such as atomic force microscopy, would be unrealistically too slow to build relevant systems in large scale. Therefore, new building procedures, such as those based on self-assembly, should be considered.

Diamondoids carry several properties which make them suitable as BBs: they have many sizes and forms, leading to several nanobrick types, and their superior stability and rigidity benefits building robust complex systems. However, diamondoids are fully hybridized with hydrogen, leading to weak intermolecular interactions, and consequently brittle crystalline structures. Functionalization could solve several of those limitations, since it generates chemically active sites, leading to stronger intermolecular interactions and stiff nanostructures. Such functionalization could also help self-assembly, driving the system to pre-determined organized configurations.

This investigation reports the physical properties of functionalized adamantane molecules with boron and nitrogen to form bora-, tetra-bora-, aza-, and tetra-aza-adamantane, using first principles calculations. We found that functionalization is strongly favorable and leads to at least two types of FBBs: tetra-bora-adamantane and tetra-aza-adamantane. In such context, we investigated a hypothetical crystalline structure, formed by a combination of those two functionalized adamantane molecules. The paper is organized as follow: section II presents the theoretical model, section III presents the properties of pure and functionalized adamantane, and section IV presents the properties of a crystalline structure formed by functionalized adamantane molecules.

II. METHODOLOGY

Theoretical modeling is an important tool to decipher the physical properties of nanostructured systems. Diamondoids have been recently investigated by first principles methodology: trends in stability and electronic properties¹¹⁻¹³, electron affinity⁵, trends in Raman spectra¹⁴, and their interaction with an atomic force microscope tip¹⁵. Diamondoid functionalization¹¹ and doping¹⁶ have also been explored. In this investigation, the properties of functionalized adamantane molecules were computed using the “Vienna *ab initio* simulation package” (VASP)¹⁷. The electronic exchange correlation potential was described with the density functional theory/generalized gradient approximation (DFT/GGA)¹⁸. The electronic wave-functions were described by a Projector Augmented Wave (PAW)¹⁹ and expanded in a plane-wave basis set, with the kinetic energy cutoff of 450 eV. Convergence in total energy was achieved when it differed by less than 0.1 meV/atom between two self-consistent iterations. The optimization of each configuration was performed until forces were

lower than 3 meV/Å.

The isolated adamantane molecules, in pure or functionalized forms, were placed in a cubic simulation cell with a fixed parameter of 17 Å and periodic boundary conditions. Such a large simulation cell guaranteed negligible interactions between the molecule and its neighboring images. The Brillouin zone was sampled by the Γ -point. The enthalpy of formation ($\Delta_f H$) of each adamantane-like molecule was computed by:

$$\Delta_f H(X_n C_{10-n} H_{16-n}) = E_{\text{tot}}(X_n C_{10-n} H_{16-n}) - nE(X) - (10 - n)E(C) - (16 - n)E(H) \quad (1)$$

where $E_{\text{tot}}(X_n C_{10-n} H_{16-n})$ is the total energy of the molecule, with n atoms of type X ($X = B, N$), $(10 - n)$ carbon, and $(16 - n)$ hydrogen atoms. The $E(X)$, $E(C)$, and $E(H)$ are the total energies, per atom, of respectively X , carbon, and hydrogen elements, in their standard states. Those energies, computed within the same methodology described in the previous paragraphs, were obtained from the total energy of carbon in a diamond lattice, nitrogen in an isolated N_2 molecule, hydrogen in an isolated H_2 molecule, and boron in a trigonal crystalline structure. This procedure has been used in several other systems to compute energies of formation^{20,21}.

The crystal, in a zincblende structure with a basis formed by tetra-bora-adamantane and tetra-aza-adamantane molecules, was simulated using the same theoretical approximations and convergence criteria described earlier for the isolated molecules. The Brillouin zone was sampled by a $8 \times 8 \times 8$ k-point grid.

III. PURE AND FUNCTIONALIZED ADAMANTANE

We discuss the properties of adamantane and the resulting changes of incorporation single and multiple boron or nitrogen atoms. There are two types of carbon atoms in adamantane, labeled C(1) and C(2). A C(1) is bound to three C(2)'s and one H atom, while a C(2) is bound to two C(1)'s and two H's. According to table I, interatomic distances and bond angles for all molecules investigated here were in excellent agreement with available experimental data²²⁻²⁵. In adamantane, the C(1)-C(2) interatomic distances are 1.538 Å, close to the respective value in crystalline diamond (1.545 Å). The C(1)-H and C(2)-H interatomic distances are 1.105 Å in average, close to typical C-H distances in organic molecules. The average C-C-C bond angles are 109.5°, indicating the sp^3 character of carbon

bonding. The H-C(2)-H bond angles are 106.9° , in agreement with another theoretical investigation (106.8°)¹⁵. The electronic gap, the difference in energy between the highest occupied molecular orbital (HOMO) and the lowest unoccupied molecular orbital (LUMO), is 5.7 eV, larger than the bandgap of crystalline diamond of 4.1 eV, computed using the same methodology. The relative difference of 39% between these two gap values is consistent with that obtained by another theoretical investigation¹¹. Figure 1a presents the relaxed structures and the respective HOMO and LUMO probability density distributions. The HOMO is related to the C(1)-C(2) plus the C(1)-H bonds, which is fully consistent with the one in hexamantane¹¹. The LUMO is related to the C(1)-C(2) bonds with an anti-bonding character, distributed in the back-bond of C(2) atoms. Enthalpy of formation is -133.2 kcal/mol, demonstrating the strong stability of adamantane.

Boron and nitrogen atoms are potential candidates to react with adamantane molecules and lead to stable FBBs. They have essentially the same atomic size of carbon, and therefore, they would cause small perturbations when incorporated in carbon sites. Functionalization in the C(1) or C(2) would provide respectively four or six active sites for intermolecular bonding. Although, a larger number of active sites would be desirable, since it could lead to stiffer nanomaterials¹⁰, there are strong evidences that functionalization with those atoms is favorable in the C(1) sites^{23,25}.

Incorporation of one nitrogen atom, replacing a C(1)-H group, to form aza-adamantane (NC_9H_{15}), leads to important changes on the properties of the original adamantane molecule. The N-C(2) interatomic distance is 1.472 Å, which is similar to the respective one in aza-diamantane, in which theoretical calculations found a value of 1.448 Å¹¹. The nitrogen atom affects very weakly the other C-C and C-H bonds. Nitrogen incorporation changes the electronic structure of adamantane by reducing the gap from 5.6 to 3.6 eV. Nitrogen has five valence electrons and forms a trigonal configuration, sharing three electrons with its neighboring C(2) atoms, and keeping two electrons in a non-bonding p_z configuration. While the HOMO is associated with this non-bonding orbital, the LUMO is essentially equivalent to that of adamantane, as shown in figure 1b. This molecule is very stable, with an enthalpy of formation of only 24.4 kcal/mol higher than that of adamantane.

Functionalization with three additional nitrogen atoms, replacing the remaining C(1)-H groups of aza-adamantane, forms the tetra-aza-adamantane molecule ($\text{N}_4\text{C}_6\text{H}_{12}$). The N-C(2) distances are equivalent to that in aza-adamantane, at 1.476 Å. The C-H inter-

atomic distances and angles are slightly affected by the inclusion of additional nitrogen atoms. In tetra-aza-adamantane, the LUMO has the same character of adamantane and aza-adamantane, while the HOMO is a degenerated state associated with the four nitrogen non-bonding orbitals. The energy cost to form tetra-aza-adamantane from adamantane is also small, since enthalpy of formation is only 84.8 kcal/mol higher than that of adamantane. This value is in excellent agreement with experimental data of 80.6 kcal/mol²⁴.

Replacing a C(1)-H group by one boron atom in adamantane forms bora-adamantane (BC₉H₁₅). Although the C-C and C-H distances are slightly affected by boron incorporation, the tetrahedral configuration of the original C(1) site is deformed, leading to a near planar configuration with a trigonal symmetry, with C(2)-B-C(2) and B-C(2)-C(1) bond angles at 116.6° and 98.1°, respectively. B-C(2) interatomic distances are 1.568 Å, in agreement with other theoretical calculations for bora-diamantane at 1.555 Å¹¹. Boron incorporation also reduces the gap of adamantane. The charge distribution of HOMO is in the interstitial region between B-C(2) bonds, while the LUMO is associated with the boron non-bonding orbital, as shown in figure 1d. Enthalpy of formation of this molecule is only 19.1 kcal/mol higher than that of adamantane. Incorporation of three boron atoms in bora-adamantane, replacing the remaining C(1)-H groups, forms tetra-bora-adamantane (B₄C₆H₁₂). HOMO and LUMO of this molecule are consistent with the ones of bora-adamantane. The enthalpy of formation of tetra-bora-adamantane is 37.5 kcal/mol higher than that of adamantane, suggesting a strong stability for this molecule, although it has not been synthesized so far.

We also simulated the bora-adamantane-aza-adamantane super-molecule (H₁₅C₉B-NC₉H₁₅), which comprises an aza-adamantane plus a bora-adamantane with a B-N intermolecular bond. This B-N bond distance is 1.737 Å, in agreement with experimental value of 1.690 Å²⁵. All other interatomic distances and bond angles (table I) are in excellent agreement with experimental data. Binding energy is 0.96 eV, showing that bonding between two functionalized adamantane molecules is much stronger than that between two pure molecules, around 0.1-0.2 eV¹¹.

IV. FUNCTIONALIZED ADAMANTANE MOLECULAR CRYSTAL

Self-assembly of complex structures using nanoparticles has received considerable attention in the literature^{10,26}. Finding appropriate BBs to allow precise and fast self-assembly

still represents a major challenge. In order to lead to stable nanostructures, the BBs should carry a number of desired properties. The resulting nanostructures should be stiff and rigid, therefore intermolecular bonding between neighboring BBs should be strong, in addition to strong intramolecular bonding. This rules out pure adamantane as a potential FBB, since intermolecular bonding is generally weak, and although a crystalline structure could be attained, it would not be enough stiff²⁷. On the other hand, functionalized adamantane could satisfy both conditions. The strong intermolecular bonding could be attained between the boron active sites in tetra-bora-adamantane and the nitrogen ones in tetra-aza-adamantane, equivalent to bonding observed in the aza-adamantane-bora-adamantane super-molecule. If those functionalized molecules were dissolved in solution, ionic interactions between the nitrogen and boron sites in different molecules could favor self-assembly with great positional precision. The resulting B←N dative bonding would likely guarantee stability and rigidity of the nanostructure up to room temperature. Larger diamondoids could also be functionalized with boron and nitrogen atoms, leading to additional building block types, allowing more freedom in building complex structures.

The tetra-bora- and tetra-aza-adamantane isolated molecules have tetrahedral symmetry and four chemically active sites, which allowed to envision a hypothetical molecular crystal in a zincblende structure ($F\bar{4}3m$ space group), with those two molecules forming the basis. Therefore, the crystal would be formed by a tetra-bora-adamantane sitting in the lattice origin with a tetra-aza-adamantane sitting in the $(1/4,1/4,1/4)a$ position, where a is the lattice parameter. Figure 2 presents a schematic representation of this molecular crystal. This crystal should be very stable, since boron and nitrogen atoms would lie in a near tetrahedral environment and any boron (nitrogen) atom in tetra-bora(tetra-aza)-adamantane would bind to one nitrogen (boron) atom in a neighboring tetra-aza(tetra-bora)-adamantane molecule. The intermolecular bonding in the crystal is essentially due to B-N interactions.

Figure 3 presents the crystal total energy as a function of the lattice parameter. The reference energy is defined for infinitely separated molecules, such that crystal formation leads to a large energy gain. We initially simulated the system by varying the lattice parameter, constraining the molecular internal degrees of freedom, such that only the B-N distances varied. This already allowed a large cohesive energy $E_c = 1.02$ eV per primitive cell at $a = 12.0$ Å. By releasing that constrain, there was a further energy gain, and $E_c = 1.81$ eV at $a = 11.45$ Å. The corresponding B-N distance is 1.907 Å, which is longer than that

in bora-adamantane-aza-adamantane super-molecule, discussed in previous section. This results from the competition among the four B←N bonds in each molecule. The internal configurations of tetra-bora-adamantane and tetra-aza-adamantane molecules in the crystal differed only slightly from those of isolated configurations. The relevant relaxations were on the tetra-bora-adamantane molecule, where the B-C bond distances and B-C-B bond angles changed from 1.589 Å and 90.1° in the isolated molecule to 1.624 Å and 102.5° in the crystal. In the crystal, boron relaxed toward a near tetrahedral configuration by interacting with neighboring nitrogen atoms.

The stiffness of the resulting crystal could be determined by its bulk modulus. We found a bulk modulus of 20 GPa, which is considerably smaller than that of typical covalent solids, that ranged from 100 GPa, in silicon, to around 400 GPa, in diamond and boron nitride. However, it is still larger than the values for other molecular crystals²⁸. Considering the small relaxation on intramolecular bonds in the molecular crystal, the materials stiffness is essentially controlled by the variations in the intermolecular B-N bonds. This is confirmed by comparing the density of B-N bonds in c-BN with that in the molecular crystal. This density is about 30 times smaller in the molecular crystal than in c-BN, being consistent with a factor of about 20 between the respective bulk moduli.

The band structure of the molecular crystal, depicted in Figure 4, shows a direct bandgap of 3.9 eV, which could be compared to 4.8 eV for the direct gap of a pure adamantane molecular crystal²⁷. Both values should be considered as lower limits, since the DFT/GGA framework generally underestimates gap energies. Corrections by those authors²⁷ led to a 44% increase in the gap, suggesting corrections to the gap of this molecular crystal could lead to a value around 5-6 eV. Figure 5 shows the probability charge distribution of the molecular crystal in the (110) plane. The top of the valence band is described as a combination of the HOMO orbitals from isolated molecules: the nitrogen non-bonding 2p orbital in tetra-aza-adamantane, that now is associated with the B←N dative bond, and the C-B orbital in the tetra-bora-adamantane units. The bottom of the conduction band is associated with the carbon atoms in the tetra-bora-adamantane molecules.

V. SUMMARY

In summary, functionalized adamantane molecules have been investigated as potential fundamental building blocks for nanostructure self-assembly. Considering the enthalpies of formation, we found that boron or nitrogen incorporation in adamantane molecules with one (aza- or bora-adamantane) and four functional groups (tetra-aza- or tetra-bora-adamantane) are very stable, although the last one has not been synthesized so far. A hypothetical molecular crystal, formed by tetra-bora-adamantane plus tetra-aza-adamantane molecules, in a zincblende structure, presented a reasonably large cohesive energy of 1.81 eV/primitive cell and bulk modulus of 20 GPa. These values are considerably larger than those in typical molecular crystals, and may provide stability and stiffness at room temperature. Any defect in this hypothetical crystal, as result of imperfect self-assembly, would likely cause only minor changes in the materials stiffness²⁹. The electronic band structure of this crystal presented a direct and wide bandgap of 3.9 eV, suggesting potential applications in opto-electronics.

Acknowledgments

The authors acknowledge support from the Brazilian Agency CNPq. The calculations were performed at the computational facilities of CENAPAD-São Paulo.

-
- ¹ P. Avouris, Z. H. Chen, and V. Perebeinos, *Nature Nanotechnology* **2**, 605 (2007).
 - ² S. J. Tans, A. R. M. Verschueren, and C. Dekker, *Nature (London)* **393**, 6680 (1998).
 - ³ X. L. Li, X. R. Wang, L. Zhang, S. W. Lee, and H. J. Dai, *Science* **319**, 1229 (2008).
 - ⁴ J. E. Dahl, S. G. Liu, and R. M. K. Carlson, *Science* **299**, 96 (2003).
 - ⁵ N. D. Drummond, A. J. Williamson, R. J. Needs, and G. Galli, *Phys. Rev. Lett.* **95**, 096801 (2005).
 - ⁶ W. L. Yang *et al.*, *Science* **316**, 1460 (2007).
 - ⁷ S. Basu, W. P. Kang, J. L. Davidson, B. K. Choi, A. B. Bonds, and D. E. Cliffler, *Diam. Relat. Mater.* **15**, 269 (2006).
 - ⁸ Z. D. Wang, S. A. Stout, and M. Fingas, *Environmental Forensics* **7**, 105 (2006).
 - ⁹ J. R. Schnell and J. J. Chou, *Nature (London)* **451**, 591 (2008).
 - ¹⁰ R. C. Merkle, *Nanotechnology* **11**, 89 (2000).

- ¹¹ G. C. McIntosh, M. Yoon, S. Berber, and D. Tománek, Phys. Rev. B **70**, 045401 (2004).
- ¹² A. J. Lu, B. C. Pan, and J. G. Han, Phys. Rev. B **72**, 035447 (2005).
- ¹³ Y. Y. Wang *et al.*, Nature Materials **7**, 38 (2008).
- ¹⁴ J. Filik, J. N. Harvey, N. L. Allan, P. W. May, J. E. P. Dahl, S. Liu, and R. M. K. Carlson, Phys. Rev. B **74**, 035423 (2006).
- ¹⁵ G. P. Zhang, T. F. George, L. Assoufid, and G. A. Mansoori, Phys. Rev. B **75**, 035413 (2007).
- ¹⁶ A. S. Barnard, S. P. Russo, and I. K. Snook, J. Chem. Phys. **118**, 10725 (2003).
- ¹⁷ G. Kresse and J. Furthmüller, Phys. Rev. B **54**, 11169 (1996).
- ¹⁸ J. P. Perdew, K. Burke, and M. Ernzerhof, Phys. Rev. Lett. **77**, 3865 (1996).
- ¹⁹ G. Kresse and D. Joubert, Phys. Rev. B **59**, 1758 (1999).
- ²⁰ L. V. C. Assali, W. V. M. Machado, and J. F. Justo, Phys. Rev. B **69**, 155212 (2004).
- ²¹ R. Larico, J. F. Justo, W. V. M. Machado and L. V. C. Assali, Phys. Rev. B **79**, 115202 (2009).
- ²² V. Vijayakumar, A. B. Garg, B. K. Godwal, and S. K. Sikka, J. Phys.-Condens. Matter. **13**, 1961 (2001).
- ²³ S. P. Kampermann, T. M. Sabine, B. M. Craven, and R. K. McMullan, Acta Cryst. A **51**, 489 (1995).
- ²⁴ M. Mansson, N. Rapport, and E. F. Westrum, J. Am. Chem. Soc. **92**, 7296 (1970).
- ²⁵ Yu. N. Bubnov, M. E. Gurskii, D. G. Pershin, K. A. Lyssenko, and M. Y. Antipin, Russ. Chem. Bull. **47**, 1771 (1998).
- ²⁶ C. R. Iacovella and S. C. Glotzer, Nano Lett. **9**, 1206 (2009).
- ²⁷ T. Sasagawa and Z.-X. Shen, J. Appl. Phys. **104**, 073704 (2008).
- ²⁸ G. M. Day, S. L. Price, and M. Leslie, Crystal Growth Design **1**, 13 (2001).
- ²⁹ T. Dumitrica and B. I. Yakobson, Phys. Rev. B **72**, 035418 (2005).

TABLE I: Properties of adamantane in pure ($C_{10}H_{16}$) and functionalized forms (BC_9H_{15} , $B_4C_6H_{12}$, NC_9H_{15} , $N_4C_6H_{12}$, and $H_{15}C_9B-NC_9H_{15}$). The table presents the average bond angles (A) and distances (d) between C(1)-C(2) and C(2)-X atoms, where X is C(1), B or N in pure, boron or nitrogen functionalized molecules, respectively. ΔE_{H-L} is the HOMO-LUMO energy difference and $\Delta_f H$ is the enthalpy of formation, with adamantane as the reference. Distances, angles, energies, and enthalpies of formation are given in Å, degrees, eV, and kcal/mol, respectively. Experimental data are given in parenthesis.

	$B_4C_6H_{12}$	BC_9H_{15}	$C_{10}H_{16}$	NC_9H_{15}	$N_4C_6H_{12}$	$H_{15}C_9B-NC_9H_{15}$	
	X = B	X = B	X = C(1)	X = N	X = N	X = B	X = N
d[C(1)-C(2)]	–	1.552	1.538	1.539	–	1.543	1.537
			(1.53) ^(a)			(1.536) ^(d)	(1.534) ^(d)
d[C(2)-X]	1.589	1.568	–	1.472	1.476	1.634	1.504
					(1.473) ^(b)	(1.626) ^(d)	(1.503) ^(d)
A[C-C-C]	–	110.6	109.5	108.8	–	110.1	109.2
			(109.45) ^(a)			(110.1) ^(d)	(109.6) ^(d)
A[C(2)-X-C(2)]	117.2	116.6	–	109.5	107.8	108.8	108.1
					(108.0) ^(b)	(108.6) ^(d)	(108.0) ^(d)
A[X-C(2)-C(1)]	–	98.1	–	111.6	–	107.5	112.1
						(107.8) ^(d)	(112.5) ^(d)
A[X-C(2)-X]	90.1	–	–	–	112.8	–	–
					(112.6) ^(b)		
A[H-C(2)-H]	112.0	106.6	106.9	107.1	108.4	106.5	107.5
					(110.7) ^(b)		
ΔE_{H-L}	2.3	4.8	5.7	3.7	4.4	4.1	
$\Delta_f H$	37.5	19.1	0	24.4	84.8	21.2	
					(80.6) ^(c)		

^(a) Reference²², ^(b) Reference²³, ^(c) Reference²⁴, ^(d) Reference²⁵.

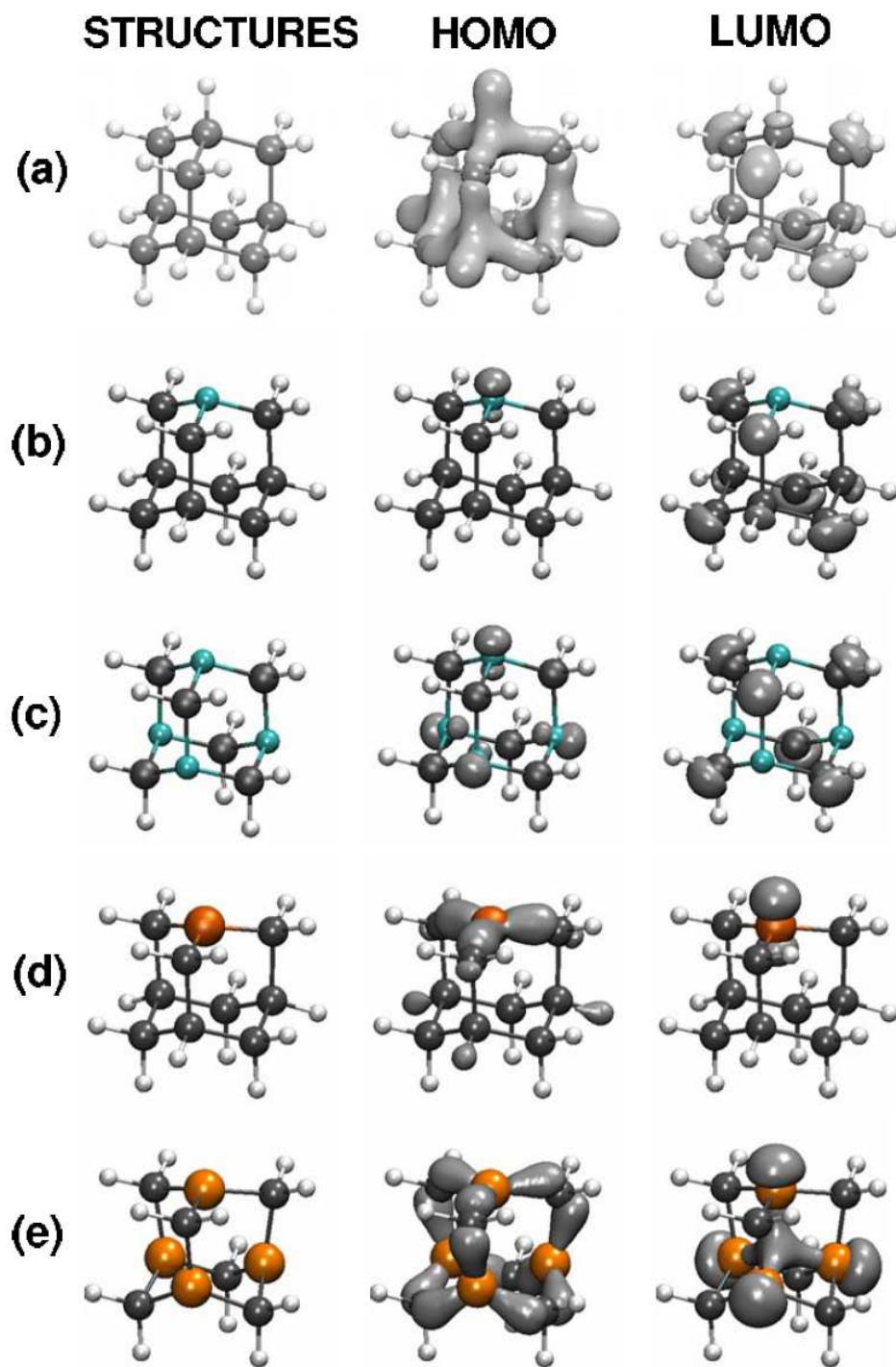


FIG. 1: (Color online) Optimized molecular structures and probability density isosurfaces of HOMO and LUMO in: (a) adamantane, (b) aza-adamantane, (c) tetra-aza-adamantane, (d) bora-adamantane, and (e) tetra-bora-adamantane. Black, light gray (blue), dark gray (orange), and white spheres represent carbon, nitrogen, boron, and hydrogen atoms, respectively. Each isosurface corresponds to 30% of the respective maximum probability.

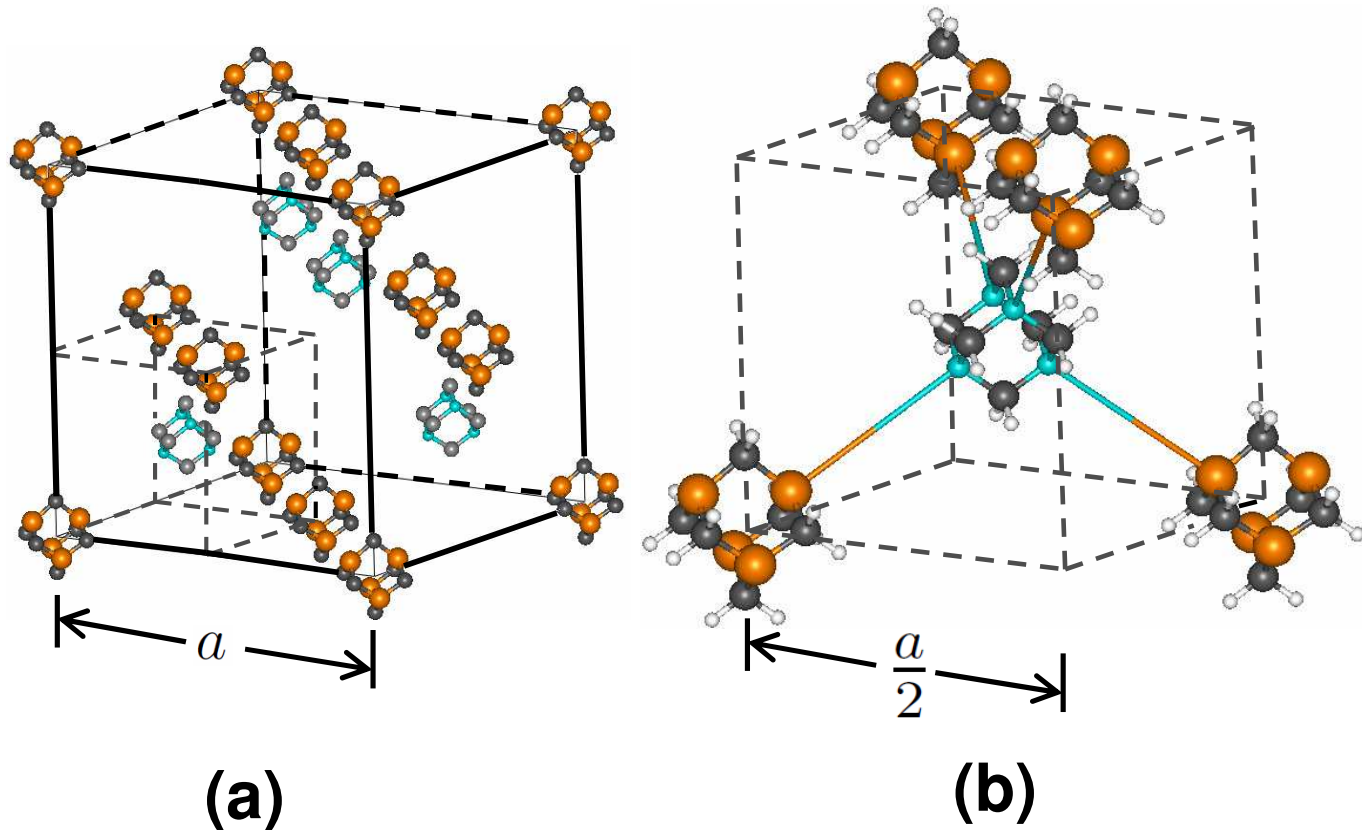


FIG. 2: (Color online) Schematic representation of: (a) the zincblende structure of the molecular crystal, composed of a tetra-bora-adamantane in the origin plus a tetra-aza-adamantane in the $(1/4,1/4,1/4)a$ position, where a is the lattice parameter; (b) the tetrahedral intermolecular B-N bonds. For clarity, hydrogen atoms were removed in (a). (Coloring of spheres is consistent with that in figure 1.)

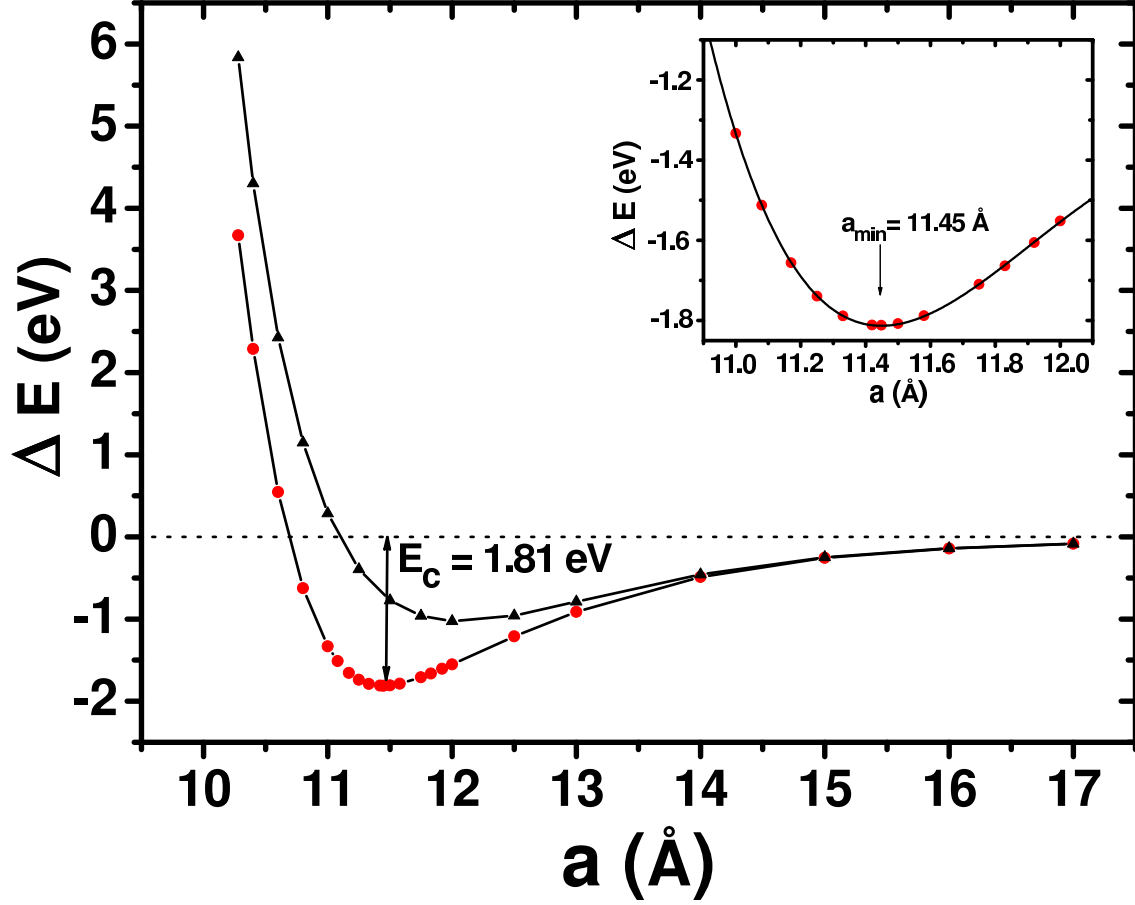


FIG. 3: Total energy variation (ΔE) of the tetra-aza-adamantane plus tetra-bora-adamantane crystal, with respect to infinitely separated molecules, as a function of the lattice parameter a , with (dots) and without (triangles) relaxation of the molecular internal degrees of freedom. The inset shows the energy close to the minimum for the crystal with full relaxation.

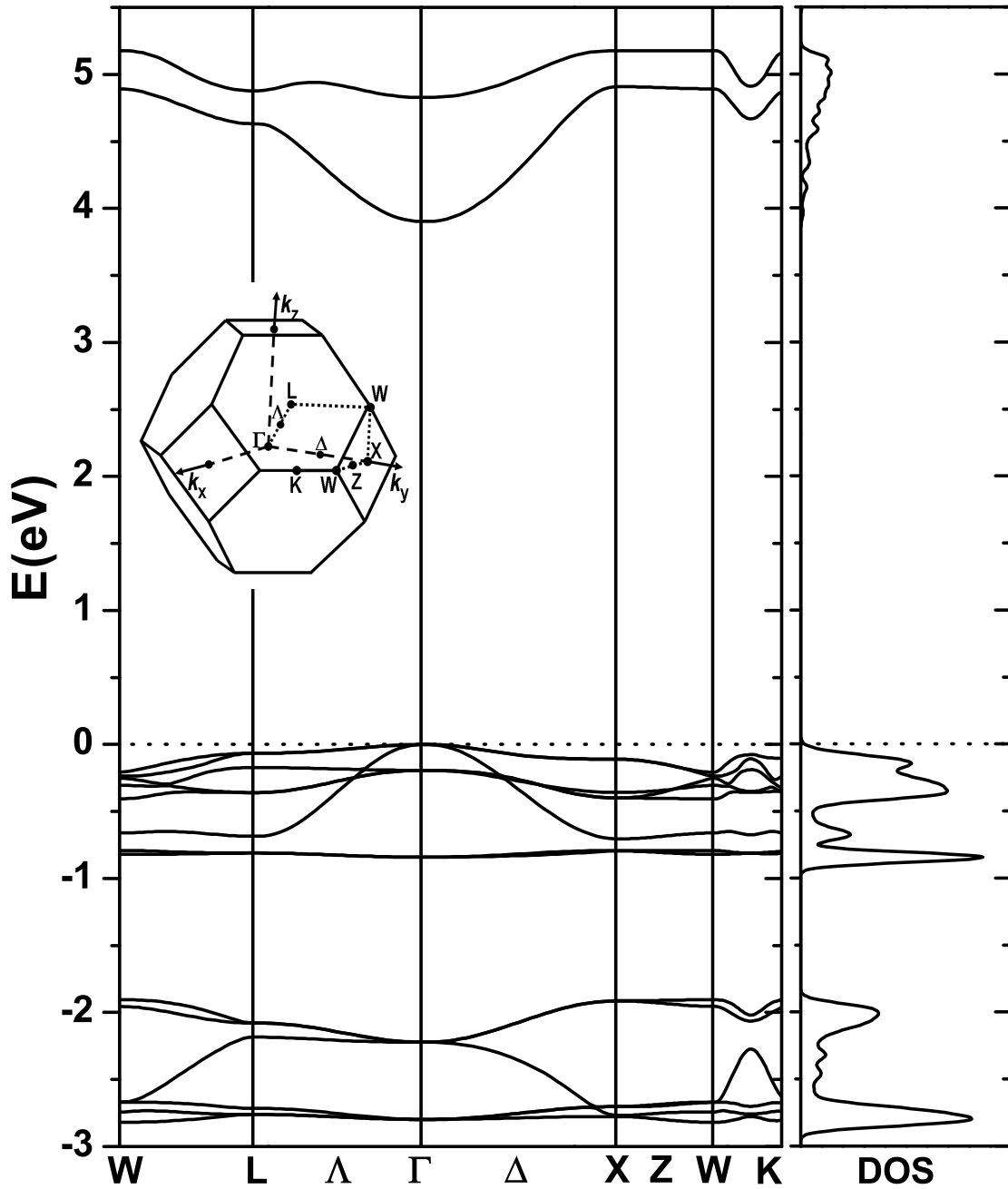


FIG. 4: Energy band structure along several high symmetry directions and density of states (DOS) of the molecular crystal schematically represented in figure 2. The inset shows the first Brillouin zone and the respective high symmetry points.

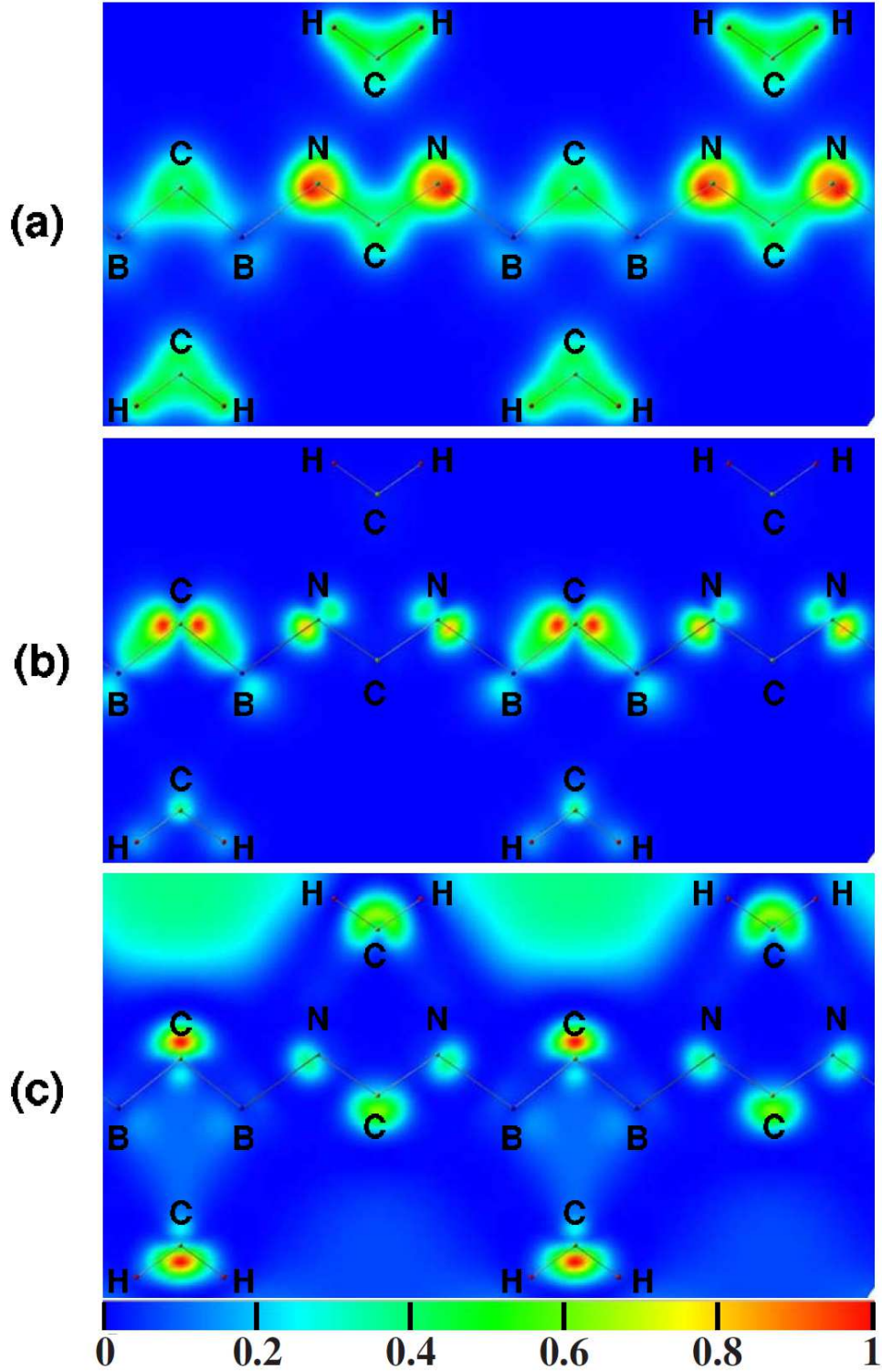


FIG. 5: (Color online) Density probability isosurfaces in the (110) plane for the molecular crystal: (a) total charge, (b) top of the valence band, and (c) bottom of the conduction band. The results are represented with respect to the maximum density probability (ρ_{max} in $e/\text{\AA}^3$): (a) $\rho_{max} = 4.13$, (b) $\rho_{max} = 0.54$, and (c) $\rho_{max} = 0.06$.